The role of actin cables in directing the morphogenesis of the pharyngeal pouches

Robyn Quinlan[1], Paul Martin[2,*] and Anthony Graham[1,†]

[1]MRC Centre for Developmental Neurobiology, 4th Floor New Hunts House, Guys Campus, Kings College London, London SE1 1UL, UK
[2]Department of Anatomy and Developmental Biology, University College London, Gower Street, London WC1E 6BT, UK
*Present address: Departments of Physiology and Biochemistry, University of Bristol, School of Medical Sciences, University Walk, Bristol BS8 1TD, UK
†Author for correspondence (e-mail: anthony.graham@kcl.ac.uk)

Accepted 27 October 2003

Development 131, 593-599
Published by The Company of Biologists 2004
doi:10.1242/dev.00950

Summary

The pharyngeal arches are separated by endodermal outpocketings, the pharyngeal pouches. These are structures of considerable importance; they are required to segregate the mesenchymal populations of each arch and to induce the formation of arch components, and they generate specific derivatives, including the parathyroid and the thymus. The pharyngeal pouches are first evident as localised sites at which the endoderm contacts the ectoderm, and they then expand along the proximodistal axis to generate the narrow, tight morphology of the mature pouch. We currently have no knowledge of the morphogenetic mechanisms that direct formation of the pharyngeal pouches. Here, in chick, we show that cells within the pharyngeal pouch endoderm have an abundance of apically located actin fibres that are networked within the endodermal sheet, via their insertion into N-cadherin adherens junctions, to form a web of supra-cellular actin cables. Cytochalasin D disruption of these actin structures results in the formation of aberrant pouches that fail to generate their normal slit-like morphology. This suggests that the process of pharyngeal pouch morphogenesis involves the constraining influence of these actin cables that direct expansion, within the pouch, along the proximodistal axis. These results, importantly, provide us with vital insights into how the pharyngeal pouches form their normal morphology. They also give evidence, for the first time, of actin cables functioning as constraints during complex vertebrate morphogenetic episodes.

Key words: Pharyngeal pouches, Pharyngeal endoderm, Actin cables, Morphogenesis, Chick

Introduction

The pharyngeal arches are evident as a series of bulges found on the lateral surface of the head of all vertebrate embryos, and it is within these that the nerves, muscle, skeleton and epithelia of the pharynx originate and differentiate. Significantly, the development of this territory is extremely complex involving interactions between a number of disparate embryonic cell types: ectoderm, endoderm, mesoderm and neural crest, each of which generates particular components of the arches, and whose development must be coordinated to generate the functional adult oro-pharyngeal apparatus (Graham and Smith, 2001).

Previous studies have, for a number of reasons, tended to focus on the role of the neural crest in guiding the development of the pharyngeal arches (Graham et al., 1996). We are, however, gaining a greater understanding of how the pharynx is constructed and it is now clear that our previous ideas must be reassessed. In particular, it is becoming apparent that the neural crest plays a less pervasive role than was previously believed, and that much of the development of the pharynx is dependent upon cues from the endoderm. Importantly, we have recently shown, using ablation experiments in the chick, that pharyngeal arches can form, are regionalised and have a sense of identity in the absence of neural crest (Veitch et al., 1999). Indeed, an event that presages pharyngeal arch formation is the development of the pharyngeal pouches, and it is likely that it is these structures that play a central role in arch development. The pharyngeal pouches are first evident as outpocketings of the endoderm, which contact the ectoderm. At these defined points, the ectoderm and endoderm remain in intimate contact and expand along the proximodistal axis (Fig. 1). They thus come to separate the neural crest and mesodermal cells of the arches and to define the anterior and posterior limits of each arch. The pouches also act to induce the formation of particular arch components, such as the epibranchial placodes (Begbie et al., 1999), and themselves generate specific derivatives, including the parathyroid and thymus. Significantly, in the zebrafish mutant *vgo*, in which the pharyngeal pouches fail to form, pharyngeal arch development is severely perturbed (Piotrowski and Nusslein-Volhard, 2000).

Although the pharyngeal pouches are important, we know very little about how their morphogenesis is directed. It is clear that this must involve a remodelling of the endoderm, such that the initial outpocketing that defines the pouch elaborates along the proximodistal axis, adopting a narrow slit-like morphology. Interestingly, studies into a variety of other morphogenetic episodes in both vertebrates and invertebrates (Jacinto et al., 2001) have described the involvement of actin cables that

function at the level of the tissue to bring about specific movements. We have therefore analysed whether such actin structures are associated with the pharyngeal pouches and, if so, what role they may play in directing their morphogenesis. We have found that actin cables, linked via N-cadherin adherens junctions, are indeed a feature of the pouch endoderm as it is undergoing proximodistal expansion. Furthermore, we have also demonstrated that if these cables are disrupted, the pouches fail to generate their normal morphology; thus we propose that these cables are required to act as constraints directing the growth of the pouches along the proximodistal axis.

Materials and methods

In situ hybridisation

Chick eggs were incubated at 38°C in a humid atmosphere, staged according to Hamilton and Hamburger (Hamburger and Hamilton, 1951) and fixed overnight at 4°C in MEMFA. In situ hybridisation was performed as described by Henrique et al. (Henrique et al., 1995). The probes used have all been described previously: *Bmp7*, *Pax1*, *Dlx2* and N-cadherin. Following in situ hybridisation, embryos were either bi-sected and mounted under 90% glycerol, or embedded in gelatin-albumin with 2.5% glutaraldehyde and vibratome sectioned at 50 μm.

Wholemount phalloidin staining and immunohistochemistry

MEMFA-fixed embryos were washed in PBS + 1% Triton X-100 (PBSTx). For phalloidin staining of f-actin, embryos were incubated overnight at 4°C with 6.6 nM Alexa-Fluor 488 Phalloidin (Molecular Probes). For nuclear staining, embryos were briefly washed in 2×SSC (pH 7.0) + 1% Triton X-100, treated with RNase A (1 mg/ml) for 30 minutes at 37°C, then incubated with propidium iodide (100 ng/ml) either 40 minutes on the bench or overnight with phalloidin at 4°C. For analysis of N-cadherin protein, embryos were first blocked with PBSTx + 10% heat-treated serum, incubated for 5-7 days with anti-chicken N-cadherin antibody (R&D Systems) diluted 1:500, then washed in PBSTx + 1% serum before adding Alexa-Fluor 568 goat-anti-rat IgG conjugate diluted 1:250, overnight at 4°C. Where actin and N-cadherin double images were required, the above protocols were followed with the phalloidin staining performed last.

Confocal analysis of fluorescently labeled embryos

Embryos were washed in PBSTx, then mounted whole under coverslip with Prolong Anti-Fade (Molecular Probes). Some embryos were first embedded in 20% gelatin:PBS, the gelatin block fixed in 4% PFA + 0.01% glutaraldehyde overnight at 4°C, then vibratome-sectioned at 50-70 μm. Optical sections were collected on a Leica DMRE and a Olympus FluoView FV500 laser-scanning microscope.

Transmission electron microscopy

Embryos were collected and immediately fixed for approximately 4 hours at 4°C in 2.5% glutaraldehyde in 0.2 M phosphate buffer (pH 7.3), to which 6.6 nM phalloidin had been added to help stabilise the actin filaments. Embryos were then washed in a phosphate buffer, post-fixed in osmium tetroxide, dehydrated through an ethanol series and embedded in resin. Ultra-thin sections were cut and mounted on 200 mesh grids, and these stained with uranyl acetate and lead citrate before being viewed in a Hitachi H7600 transmission electron microscope.

Cytochalasin D treatment

A 100 mM stock solution of Cytochalasin D (Sigma) was prepared in dimethylsulphoxide (DMSO). This was further diluted in DMSO and then sterile Howard's Ringer to the required concentration. For delivery, chick eggs were windowed and staged by injecting Pelikan 17 black ink under the blastoderm. Two delivery methods were employed: beads soaked in 10 mg/ml cytochalasin D, which were introduced into the pharyngeal cavity via the hindbrain, or; direct injection of reagent into the pharyngeal cavity. For injection, final cytochalasin D concentrations of 1 mM, 100 μM and 10 μM were assessed, but phenotypes described here were generated at 100 μM cytochalasin D. All injection solutions had Fast Green dye added (1:10) to visualise delivery of the solution. Typically a 0.4 nl volume of solution was delivered by microinjection, either through the hindbrain, for embryos up to approx. stage 12, or for older embryos, through individual pouches on the right-hand side. For both delivery methods, control embryos were generated using undiluted DMSO. Embryos were either collected immediately or the eggs resealed and incubated for up to 20 hours. On collection, all embryos were fixed in MEMFA and either processed for in situ hybridisation or phalloidin staining.

Results

The morphogenesis of the pharyngeal pouches can be readily followed through the expression of *Bmp7*, which labels each of the pouches from their earliest stages (Veitch et al., 1999). Pouches form sequentially over a protracted period; by stage 12 the two most anterior pouches are just evident as localised outpocketings that bring the endoderm into close contact with the overlying ectoderm (data not shown). By stage 14, the first and second pouches have begun to elongate along the proximodistal axis (Fig. 1A). The presence of the third pouch is evident by stage 15, and like the first two, it continues to expand proximodistally as development proceeds (Fig. 1B,C). Finally, the fourth pouch forms by stage 19 (data not shown). Interestingly, we have found that staining of whole embryos with fluorescently tagged phalloidin clearly reveals a pronounced and localised accumulation of f-actin within each of the pouches, coincident with their shape change. This abundance of actin is evident within the endoderm of each pouch throughout the prolonged period of their proximodistal expansion, which occurs over an ~20-hour period. Thus at stage 14, it is apparent at the apical surface of the first and second pouches (Fig. 1D) and by stage 16, it is also apparent along the apical surface of the third pouch (Fig. 1E,F). The nature of its organisation is readily appreciated when viewed at high magnification, with actin fibres seemingly forming a supra-cellular 'cable' that assembles at the apical margin of the cells of the pouch endoderm (Fig. 1G). A longitudinal section through the pharyngeal region of a stage 18 embryo further reveals this actin structure following the lumenal contours of the pharyngeal endoderm (Fig. 1H). It is clear from Fig. 1G, which is a side view of the pouch endoderm, and Fig. 1H, which views pouch endoderm in longitudinal section, that this localised abundance of actin does not represent a simple cable within one plane of the endoderm. Instead, the actin is organised into a two-dimensional 'web' of supracellular actin cables that runs just below the apical plasma membrane of the pharyngeal endodermal cells. Importantly, this web of actin is not found throughout the pharyngeal endoderm, but instead shows a marked localised accumulation, being most abundant in regions where pouches are forming and generally at much lower abundance in the interpouch endoderm (Fig. 1H).

Supracellular actin cables have been described in other

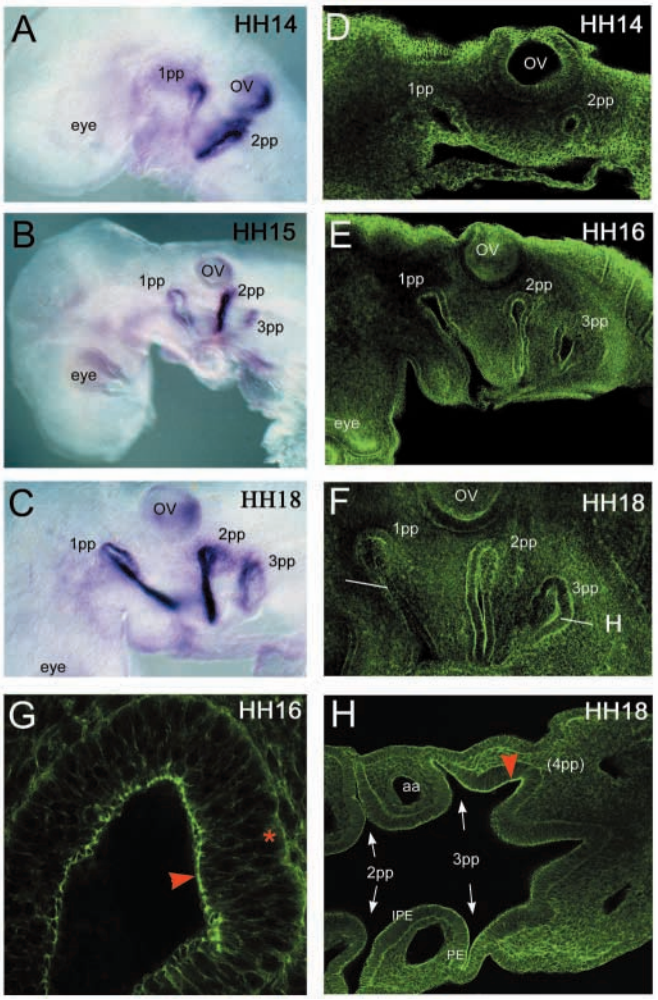

Fig. 1. The pharyngeal pouch endoderm supports a two-dimensional web of supra-cellular actin cables. Side views of embryos (A-F) where *Bmp7* expression (A-C) within the pharyngeal pouch endoderm has been used to highlight the elaboration of pouches along the proximodistal axis and phalloidin staining (D-F) has been used to visualise f-actin within the pouch endoderm. (A) At stage 14, two pharyngeal pouches (1pp and 2pp) have formed and begun to elongate along the proximodistal axis. (B) At stage 15, the third pharyngeal pouch (3pp) is evident. (C) At stage 18, all three pouches (1pp, 2pp and 3pp) have further elongated and display typical narrow slit-like pouch morphology. (D-F) Localised accumulation of actin is seen within the endoderm of each pouch as they undergo proximodistal elongation. (G) High magnification view of the third pharyngeal pouch (3pp) shows actin organised into a supracellular actin cable (red arrowhead), assembled along the apical margin of the endodermal cells (basal margin indicated by an asterisk). (H) Longitudinal section through the pharyngeal region, (at level indicated in F), showing pouches as distinct outpocketings of endoderm. The pharyngeal endoderm is described as pouch endoderm (PE) or interpouch endoderm (IPE). A two-dimensional web of supracellular cables, which follows the lumenal contours of the pouch endoderm, appears to be localised to regions where pouches are forming (red arrowhead) or have just formed, but at lower abundance in the interpouch endoderm (IPE). OV, otic vesicle; aa, arch artery. Anterior is towards the left.

systems, most notably in wounded epidermis and in dorsal closure of the epithelia of *Drosophila* embryos (Jacinto et al., 2001). Importantly, in both these instances the actin cable is able to function as a contractile purse-string, extending the full circumference of the epithelial hole, and acting to close these holes over a narrow time window of ~2 hours. The actin structures observed within pouch endoderm are not being used to close epithelia. Indeed, neither do they fully circumscribe either a pouch (Fig. 1G) nor the pharyngeal endoderm per se (Fig. 1H); instead, they accumulate within regions of the endoderm that are undergoing morphological change to form the pouches. The variable distribution of these structures would be consistent with this web of actin cables being involved, over a protracted period of around 20 hours in a progressive remodelling of the endoderm along all three axes to generate the complex three-dimensional shape of the final pouch structure.

To further detail the supracellular organisation of the actin, we analysed the pouch endoderm using TEM. This clearly reveals the presence of apically located filaments connecting via cellular junctions, morphologically similar to adherens junctions (Fig. 2A). More specifically, we show that it is N-cadherin based adherens junctions, which are associated with the actin structures. *N-cad* expression has been previously described in a number of other tissues, including the neural tube and somites (Hatta et al., 1987); however, we detail its expression within pharyngeal endoderm and show, by its strong expression within the pouch but not interpouch regions (Fig. 2B,C), its association with pouch morphogenesis. Additionally, transverse sections through pharyngeal regions reveal that *N-cad* mRNA is also distinctly localised to apical regions of the pouch endoderm (Fig. 2D). To demonstrate that the actin fibres are inserting into N-cadherin adherens junctions, we analysed embryos using both phalloidin and anti-N-cadherin antibody. A side view of a stage 18 embryo (Fig. 2E) shows actin and N-cadherin co-localised at the apical surface of each pouch. Higher magnification further demonstrates that the actin fibres are joined via N-cadherin adherens junctions (Fig. 2F). In keeping with our observations on actin deployment within the pharyngeal endoderm, we found that the N-cadherin protein was most strongly evident within regions of the endoderm where pouches were forming, or had just formed. Thus, at stage 16, the highest levels of N-cadherin protein is seen in the forming third pouch endoderm (Fig. 2G). Interestingly, in transverse section it is apparent that, like its mRNA, N-cadherin is only found in pouch and not in the interpouch endoderm (Fig. 2H,I).

To test the function of this web of supracellular actin cables in pouch morphogenesis, we targeted the pharyngeal endoderm by introducing cytochalasin D, which inhibits the new assembly of actin filaments (Urbanik and Ware, 1989), into the pharyngeal lumen. To assess the effect of cytochalasin D treatment on the actin assemblies, embryos (n=21) were treated for up to 6 hours before being fixed, stained with phalloidin and then analysed using confocal microscopy. It was apparent in all embryos treated in this manner that the supracellular cables had been severely disrupted, and that these continued to be affected for as long as 6 hours after treatment. Fig. 3A shows an embryo that was treated at stage 14– and then allowed to develop for a further 5 hours. The morphology of each of the pouches is clearly affected: the first pouch appears contorted and the second and third pouches are rounded rather than having a narrow and slit-like shape. Fig. 3B shows a higher

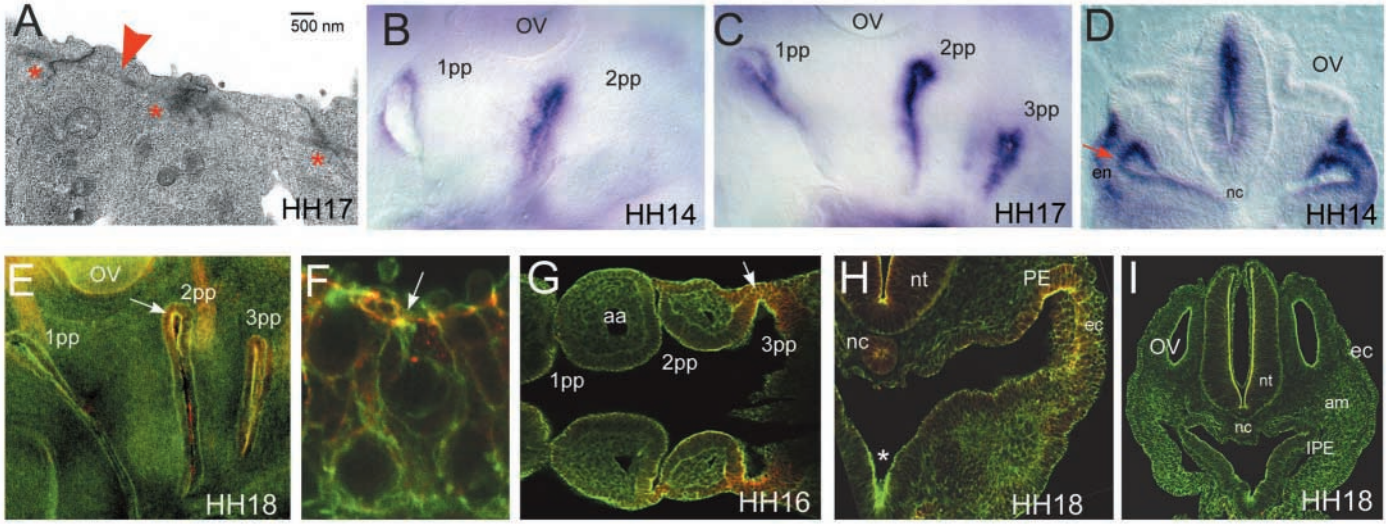

Fig. 2. The actin cables are networked within pouch endoderm via insertion into N-cadherin adherens junctions. The cellular junctions connecting the actin fibres into supracellular cables were characterised using (A) TEM, (B-D) N-cadherin in situ hybridisation, and (E-I) confocal analysis of phalloidin-stained f-actin (green) and anti-N-Cadherin antibody (red). (A) TEM image of the apical margin of cells within pouch endoderm (stage 17), showing a bundle of filaments (red arrowhead) running across the cells, just below the plasma membrane, and connecting via adherens junctions (*). (B,C) Side views showing *N-cadherin* expression within pouch endoderm of 1pp and 2pp at stage 14 (B) and 1pp, 2pp and 3pp at stage 17 (C). (D) Transverse section through second pouch (2pp) (stage 14); *N-cadherin* expression is localised to the apical surface of the pouch endoderm (red arrow). (E) Side view of a stage 18 embryo showing co-localisation (yellow) of actin (green) and N-cadherin protein (red) at the apical margin of each pouch (white arrow). (F) High magnification view of pouch endoderm showing N-cadherin protein (red) localised to the cellular junctions (white arrow) that support the actin cable (green). (G) Longitudinal section through a stage 16 embryo, showing an abundance of N-cadherin protein (red) in the last-to-form pouch (3pp) endoderm (white arrow). (H,I) Transverse confocal sections through a stage 18 embryo at the level of (H) the third pouch, indicating the pouch endoderm (PE) and (I) at lower magnification at the level of the second arch and therefore the interpouch endoderm (IPE). N-cadherin protein is found in the lateral endoderm of the pouch (PE in H), but is not apparent in the ventral pharyngeal endoderm (asterisk in H), or the interpouch endoderm (IPE in I). OV, otic vesicle; *en*, endoderm; nc, notochord; aa, arch artery; nt, neural tube; am, arch mesenchyme; ec, ectoderm. Anterior is towards the left.

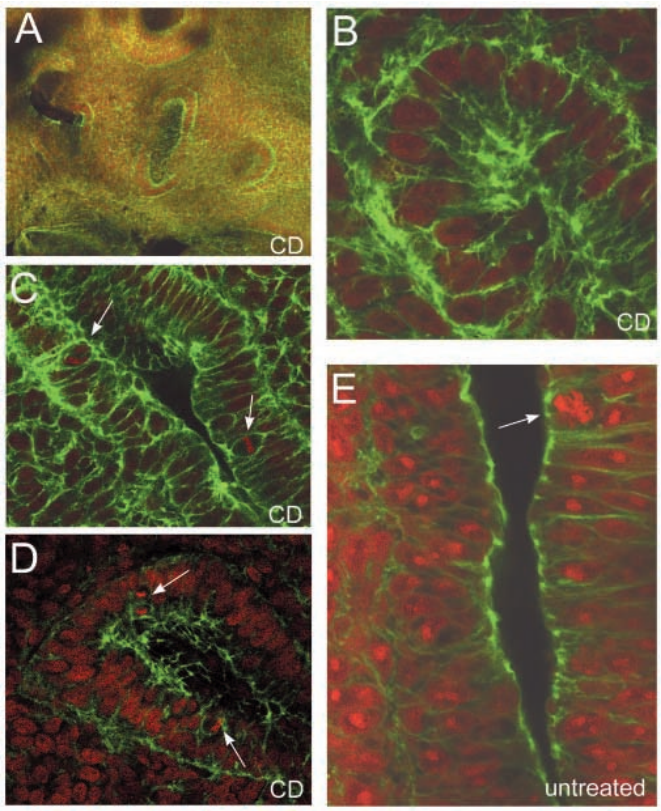

magnification view of the second pouch of a different embryo treated as before; in this specimen, actin within the dorsal tip endoderm is clearly disorganised and the supracellular cable appears to be lost. These defects are not seen in untreated embryos (Fig. 1, Fig. 3E) nor in DMSO treated controls (n=9) (data not shown). Notably, at the concentrations of cytochalasin D used here, cell proliferation has not been blocked. At a gross level, the embryos have increased in size and, more specifically, when these specimens were stained with a number of different nuclear stains (such as propridium iodide

Fig. 3. Cytochalasin D results in disorganized fibres that fail to form a coherent actin cable. Confocal analysis of phalloidin-stained f-actin (green) and propridium iodide (red) was used to assess the effects of cytochalasin D on the organisation of the actin structures within the pouch endoderm (A-D) compared with an untreated specimen (E), all at equivalent stages. (A) Side view of an embryo that was treated by introducing cytochalasin D-soaked bead into the pharyngeal cavity at stage 14– and incubated for a further 5 hours; already there is evidence of aberrant pouch morphology, where pouches are contorted (1pp) or 'relaxed' (2pp and 3pp). (B) High magnification of the dorsal tip of a second pouch shows that actin fibres fail to form a supracellular cable when treated with cytochalasin D; this embryo was treated by introduction of a bead into the pharyngeal cavity and incubated for a further 6 hours. (C,D) Mitotic cells (white arrows) are clearly evident within the pouch endoderm of embryos treated with cytochalasin D, either via a bead (C) or injection (D), as they are seen in the pouch endoderm of untreated embryos (E). CD, cytochalasin D. Anterior is towards the left.

and Topro-3) numerous mitotic cells were seen within pouch endoderm (Fig. 3C,D), as is normally observed in untreated embryos (Fig. 3E).

To further investigate the effects of cytochalasin D treatment on pouch morphogenesis, treated embryos (*n*=97) were incubated for longer periods (up to 20 hours) and then in situ analysed using a number of markers to highlight aspects of pouch morphology. Two different types of effects were seen dependent on the stage of pouch development when cytochalasin D was applied. Specifically, when cytochalasin D was delivered to the pharyngeal cavity prior to stage 14, and the embryo allowed to develop further, dramatic defects in pouch morphogenesis were observed. The specimens in Fig. 4A,B typify such effects; this embryo had cytochalasin D injected into the pharyngeal cavity at stage 11+ and the embryo then incubated for 20 hours to stage 15–. This approach uses the axial rotation of chick embryos at approximately stage 12 of development, whereby they turn to lie on their left hand side; thus, the highest concentrations of cytochalasin D within the cavity settle and lie over the tissue lining the left hand side of the cavity. This method provides an excellent experimental control as *n*=24/29 specimens treated in this manner had severe effects to the left hand side pouches but with contralateral pouches developing a normal morphology. By using *Bmp7* to highlight pouch morphology, it can be seen that the left hand side pouches of the embryo shown in Fig. 4A display a splayed, diamond-shaped morphology following exposure to cytochalasin D, but by contrast, there is clear evidence of three narrow slit-like pouches on its contralateral side (Fig. 4B). These effects were not seen in control embryos injected at equivalent stages with DMSO carrier alone; only minor defects were seen in these embryos with *n*=19/21 displaying normal development (Fig. 4C). Interestingly, of all embryos treated with cytochalasin D, in no instance did we find that cytochalasin D treatment resulted in a total failure to form any one of the pouches. Instead, as evident in Fig. 4A, pouches form but their growth is not directed proximodistally, and as such they fail to generate the typical narrow, slit-like morphology. It seems clear that the actin web is responsible, not for induction, but for shaping of the pouches and for the subsequent maintenance of their shape.

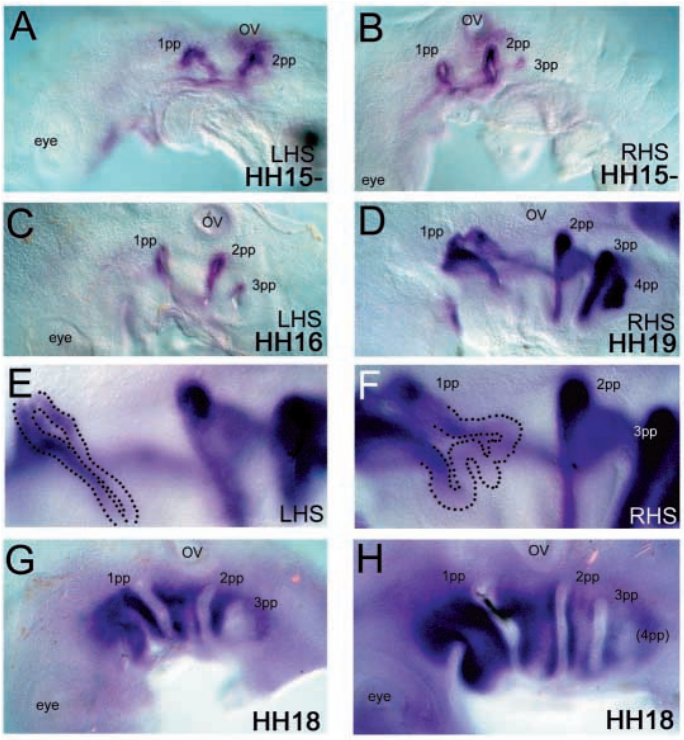

Fig. 4. Disruption of actin cable assembly results in pouches with aberrant morphology, owing to a failure in proper proximodistal elongation. Effects of cytochalasin D treatment on pouch morphogenesis analysed through (A-C) *Bmp7;* (D,F) *Pax1*; or (G,H) *Dlx2* in situ hybridization. (A,B) Left- and right-hand side views of the same embryo that had cytochalasin D injected into the pharyngeal cavity at stage 11+, prior to pouch formation, and the embryo allowed to develop to stage 15–. As the chick embryo turns, gravity causes cytochalasin D to accumulate over the left-hand side (LHS) tissue, which results in aberrant pouch morphology on that side (A) but not on the right-hand side (RHS) (B). LHS pouches have an open diamond shape compared with the narrow, slit-like pouches on the RHS or in the DMSO control (C) embryo treated in the same manner. (D) Side view of an embryo where cytochalasin D was injected into the vicinity of the first pouch (1pp) at stage 15–, and allowed to develop to stage 19. (E) High magnification of the contralateral first pouch, which did not receive an injection of cytochalasin D, displaying normal slit-like morphology. The dots outline the contours of the pharyngeal endoderm. (F) High magnification of a first pouch that did receive a cytochalasin D injection showing a contorted morphology of the pharyngeal endoderm along the proximodistal axis. Again, the dots outline the contours of the pharyngeal endoderm. (G) Side view of an embryo, treated with cytochalasin D by injection into the pharyngeal cavity at stage 12 and allowed to develop to stage 18 and (H) an embryo similarly treated with DMSO at stage 13 and allowed to develop to stage 19. In both G and H, *Dlx2* expression shows the arches have been properly populated with neural crest cells. OV, otic vesicle. Anterior is towards the left.

When cytochalasin D was injected into the pharyngeal cavity of embryos at later stages from stage 14 onwards, pouch morphology was also affected, but in a different manner in *n*=4/9 specimens. Fig. 4D shows a side view of an embryo, with pouches highlighted through *Pax1* expression (Muller et al., 1996; Veitch et al., 1999), that had received a cytochalasin D injection at stage 15– into the vicinity of the first pouch. Clearly, further pouch development has not been blocked, rather the pouch endoderm has assumed a contorted morphology, owing to growth not being directed appropriately (Fig. 4F). By contrast, the first pouch on the contralateral side, which did not receive an injection of cytochalsin D, displays the normal slit-like morphology (Fig. 4E). The effects on pouch morphology we describe here, are not simply due to an indirect effect on the pharyngeal arch mesenchyme, because in situ analysis using *Dlx2*, which labels the neural crest cells of the pharyngeal arches (Veitch et al., 1999), shows that in both experimental (Fig. 4G) and DMSO control specimens (Fig. 4H), the neural crest cells have normally populated the arches. This finding is also consistent with the fact that the neural crest are not required for normal pouch development; in the absence of crest cells pharyngeal pouches form, elongate and are normally patterned (Veitch et al., 1999). Thus, the consequences for pharyngeal morphogenesis, resulting from the direct introduction of cytochalasin D into the pharyngeal lumen, are specifically due to its disruption of

the actin cable network assembled in the cells of the pharyngeal endoderm.

Discussion

This study has analysed the role of actin in the complex morphogenesis of the pharyngeal pouches, by revealing how the actin network is organised within pharyngeal endoderm and by observing the consequences of its disruption with cytochalasin D. We show that an assembly of actin, networked by N-cadherin adherens junctions, forms supracellular cables that follow the lumenal contours of the pouch in such a way as to form a two-dimensional web-like structure. These actin cables are required for the establishment and subsequent maintenance of normal pouch morphology and we propose that one important function of these cables is in ensuring the proper proximodistal elaboration of the pouches to generate their long, slit-like shape.

Insights into the morphogenesis of the pharyngeal pouches are of crucial and timely importance. With emphasis now being placed on the role of the pouches in organising the pharyngeal apparatus as a whole (Graham, 2001), it is even more pertinent to investigate how the morphogenesis of this tissue is controlled. The results presented here provide us with the first insights into the cellular mechanisms that guide the complex morphological movements that give rise to the pharyngeal pouches. During the period of pouch morphogenesis, the pharyngeal endoderm as a whole is expanding in all directions, but the pouches themselves are primarily growing along the proximodistal axis. Importantly, it is during this period of directed proximodistal expansion that the actin cables form at the lumenal surface of the pouches. Furthermore, interfering with the actin cables during this time frame results in a failure in directed proximodistal expansion, and instead the pouches splay open or, if inhibited at later stages, have a randomly contorted shape. More specifically, these results suggest these actin cables are functioning as a constraining force upon the endodermal sheet directing the pouches to primarily elongate along the proximodistal axis and thus generate their typical narrow, slit-like shape. Besides directing the proximodistal expansion of the pouches, the actin cables could also act to give rigidity to the pouch endoderm. For instance, in a growing sheet, the rigidity afforded by the actin cables would prevent random buckling caused by the tissue taking up a shape that was simply preferred by its physical properties and those of its surrounds, thus allowing the maintenance of specific pouch shapes.

We propose that the actin network operates as a constraint within the pouch epithelium, thus forcing directed expansion and eventual slit-like morphology. A useful analogy might be to consider the effect of applying a piece of tape to a balloon as it is being inflated. Filling the balloon with air equates to increasing the number of cells within the endodermal sheet, the result being a uniform expansion of the balloon. Applying a piece of non-expanding tape to the balloon, however, constrains that region preventing a change in its surface area at this position; thus, directing expansion and generating a particular shape. Additionally, the actin cables within the pharyngeal endoderm, like the tape, act as a constraint that holds a particular shape over time, while other unconstrained areas continue to expand.

The function of actin as a constraining force within the pharyngeal endodermal sheet is a departure from the role normally ascribed to actin networks during morphogenesis, as contractile tools for drawing tissues together. However, recent studies of dorsal closure in *Drosophila* show that here too cables operate not only as purse strings, closing this hole within 2 hours, but also supply constraining forces, restricting forward movement of the leading edge, by keeping it taut and thus facilitating an orderly movement of the epithelia towards the dorsal midline (Bloor and Kiehart, 2002; Jacinto et al., 2002). It seems more accurate to view the cables as a contractile apparatus that, rather than contracting the sheet of cells, is functioning to maintain local tensions and constrain various regions in order to shape and maintain form and rigidity. Hence, it would seem that there is accumulating evidence that the constraining role for actin cables proposed here in pouch morphogenesis is a fundamental feature of actin cables during the shaping of epithelial tissues. Indeed, it is likely that actin cables functioning as constraints, particularly during vertebrate morphogenetic episodes which often involve complex three-dimensional modelling of tissues over considerably longer time periods; for example, the elongation of the pharyngeal pouches taking some 20 hours. Neural tube morphogenesis is likely to be another such example of this. For some time it has been thought that contraction of actin filaments aligned along the lumenal surface of the neuroepithelium was facilitating aspects of the elevation and fusion of the tube (Karfunkel, 1972; Lee and Nagele, 1985; Morriss-Kay and Tuckett, 1985). However, more recently it has been suggested that one function of the actin cables may be to generally maintain rigidity throughout the neuroepithelium (Ybot-Gonzalez and Copp, 1999), which would suggest that in this situation actin cables are also acting to constrain and hold shape. Furthermore, the role that we describe here for actin in constraining the morphogenesis of an epithelial sheet is also important as it is likely to be relevant to the formation of many vertebrate organs, as these also invariably involve epithelial remodelling rather than closure of a hole.

We thank Ken Brady of the EM unit at Guys Campus (KCL), for his expert assistance with the TEM study. We also thank Richard Wingate and Imelda McGonnell for constructive comments on the manuscript. This work was supported by the Medical Research Council (UK).

References

Begbie, J., Brunet, J. F., Rubenstein, J. L. and Graham, A. (1999). Induction of the epibranchial placodes. *Development* **126**, 895-902.

Bloor, J. W. and Kiehart, D. P. (2002). Drosophila RhoA regulates the cytoskeleton and cell-cell adhesion in the developing epidermis. *Development* **129**, 3173-3183.

Graham, A. (2001). The development and evolution of the pharyngeal arches. *J. Anat.* **199**, 133-141.

Graham, A. and Smith, A. (2001). Patterning the pharyngeal arches. *BioEssays* **23**, 54-61.

Graham, A., Koentges, G. and Lumsden, A. (1996). Neural crest apoptosis and the establishment of craniofacial pattern: an honorable death. *Mol. Cell Neurosci.* **8**, 76-83.

Hamburger, V. and Hamilton, H. L. (1951). A series of normal stages in the development of the chick embryo. *J. Morphol.* **88**, 49-92.

Hatta, K., Takagi, S., Fujisawa, H. and Takeichi, M. (1987). Spatial and temporal expression pattern of N-cadherin cell adhesion molecules correlated with morphogenetic processes of chicken embryos. *Dev. Biol.* **120**, 215-227.

Henrique, D., Adam, J., Myat, A., Chitnis, A., Lewis, J. and Ish-Horowicz, D. (1995). Expression of a Delta homologue in prospective neurons in the chick. *Nature* **375**, 787-790.

Jacinto, A., Martinez-Arias, A. and Martin, P. (2001). Mechanisms of epithelial fusion and repair. *Nat. Cell Biol.* **3**, E117-E123.

Jacinto, A., Wood, W., Woolner, S., Hiley, C., Turner, L., Wilson, C., Martinez-Arias, A. and Martin, P. (2002). Dynamic analysis of actin cable function during *Drosophila* dorsal closure. *Curr. Biol.* **12**, 1-20.

Karfunkel, P. (1972). The activity of microtubules and microfilaments in neurulation in the chick. *J. Exp. Zool.* **181**, 289-301.

Lee, H. Y. and Nagele, R. G. (1985). Studies on the mechanisms of neurulation in the chick: interrelationship of contractile proteins, microfilaments, and the shape of neuroepithelial cells. *J. Exp. Zool.* **235**, 205-215.

Morriss-Kay, G. and Tuckett, F. (1985). The role of microfilaments in cranial neurulation in rat embryos: effects of short-term exposure to cytochalasin D. *J. Embryol. Exp. Morphol.* **88**, 333-348.

Muller, T. S., Ebensperger, C., Neubuser, A., Koseki, H., Balling, R., Christ, B. and Wilting, J. (1996). Expression of avian Pax1 and Pax9 is intrinsically regulated in the pharyngeal endoderm, but depends on environmental influences in the paraxial mesoderm. *Dev. Biol.* **178**, 403-417.

Piotrowski, T. and Nusslein-Volhard, C. (2000). The endoderm plays an important role in patterning the segmented pharyngeal region in zebrafish (Danio rerio). *Dev. Biol.* **225**, 339-356.

Urbanik, E. and Ware, B. R. (1989). Actin filament capping and cleaving activity of cytochalasins B, D, E, and H. *Arch. Biochem. Biophys.* **269**, 181-187.

Veitch, E., Begbie, J., Schilling, T. F., Smith, M. M. and Graham, A. (1999). Pharyngeal arch patterning in the absence of neural crest. *Curr. Biol.* **9**, 1481-1484.

Ybot-Gonzalez, P. and Copp, A. J. (1999). Bending of the neural plate during mouse spinal neurulation is independent of actin microfilaments. *Dev. Dyn.* **215**, 273-283.